Speleothem-derived polycyclic aromatic hydrocarbons and monosaccharide anhydrides as tracers of past fire dynamics

Julia Homann[1], Niklas Karbach[1], Stacy A. Carolin[2], Dan James[3], David Hodell[3], Sebastian F. M. Breitenbach[4], Ola Kwiecien[4], Mark Brenner[5], Carlos Lope[6], Thorsten Hoffmann[1]

[1]Department of Chemistry, Johannes Gutenberg-Universität, Mainz, Germany
[2]School of Archaeology, University of Oxford, Oxford, UK
[3]Department of Earth Sciences, University of Cambridge, Cambridge, UK
[4]Department of Geography and Environmental Sciences, Northumbria University, Newcastle upon Tyne, UK
[5]Department of Geological Sciences, University of Florida, FL, USA
[6]Instituto Nacional de Antropología e Historia, Centro INAH Yucatán, Mérida, México

Correspondence to: Thorsten Hoffmann (hoffmant@uni-mainz.de)

Cave survey and stalagmite sample MAYA-22-7

Because only very rough scetch maps were available, our team surveyed part of Cenote Ch'en Mul in August 2022 (Fig. S1). The cenote is in direct vicinity to the Kukulcan temple and the observatory (structure Q-152) (Brown, 2006). The cenote has been targeted in archaeological studies since the Carnegie Maya project 1952-1957 (Weeks and Masson, 2009).

The cave extends from the collapse doline in north-easterly then easterly direction and results from an ancient underground stream. The overburden is only between 7 and 8 m thick and facilitates rapid infiltration. Today, the passages are characterised by large breakdown and washed-in silt- and clay-rich unconsolidated sediment. The sediment on the cave floor is rich in organic material that has been washed in during floods. Several trenches have been excavated (and filled in afterwards) in the cenote and in the main cave passage, including a trench in 1953 and two trenches called 'Bernard Trench' (Brown, 2006).

Hell Chamber in the north-eastern section of the cave hosts a large colony of bats and manifold centipedes and millipedes, crickets and other cave dwellers. Maya potsherds are widespread in all passages, indicating human activity in the past. While the main passage is largely devoid of secondary cave carbonates (speleothems), the side passages are very well decorated with stalagmites and stalactites. During our visit in 2022 the cave showed active dripping in only few places, especially in the SE, where a small puddle was detected which might be linked to the water table.

Stalagmite MAYA-22-7 (Fig. 1) was found a few meters above the puddle. It was active (i.e., dripwater was falling onto it) when it was collected. The stalagmite was packed in a large plastic zip-lock bag before being detached from the growth spot to avoid contamination of the youngest surface.

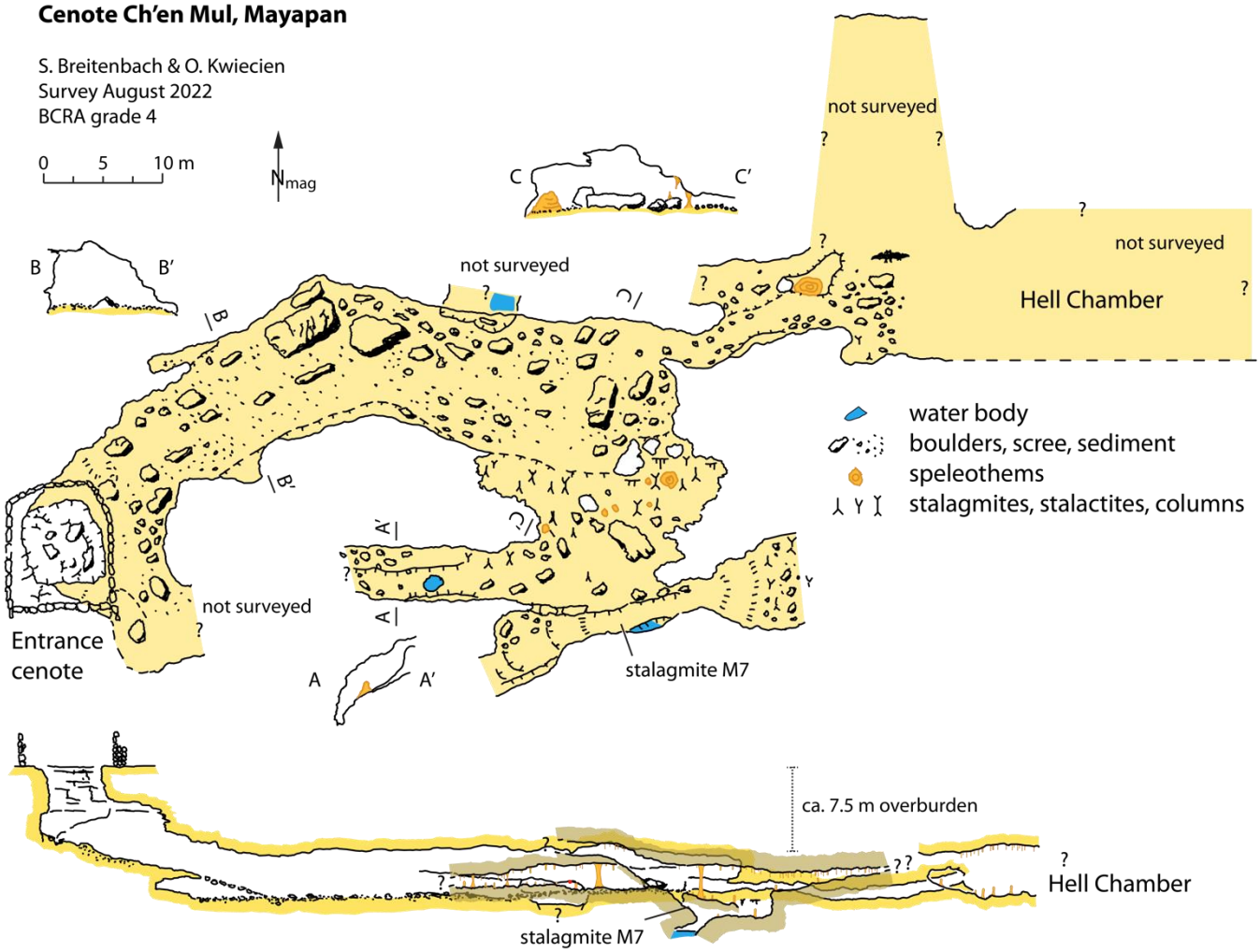

Figure S1: Map and profile of Cenote Ch'en Mul below the Mayapan ruins. The survey, conducted in August 2022, is incomplete due to time constraints. The cave passages extend below the prominent structure Q-152, which is also called Observatory (Brown, 2006). Significant additional passages remain currently unmapped.

35

OxCal Deposition model input code

Below is the code used to run the OxCal Poisson-Process Deposition model. Boundaries were placed at 14 mm and 24 mm distance from top, where there are clearly visible detrital layers in the stalagmite. A top boundary at 0 mm distance from top was input as a date between 2010-2022 CE, uniform distribution.

```
Plot()
 {
  P_Sequence("M7",0.1,null,U(-2,2))
  {
   timescale="UTh";
   Boundary();
   Date("bh03",N(calBP(332),11.5))
   {
    z=121;
   };
   Date("bh01",N(calBP(233),7))
   {
    z=90.3;
   };
   Date("bh05",N(calBP(100),6.2))
   {
    z=53.3;
   };
   Date("bh02",N(calBP(22),5.4))
   {
    z=27.3;
   };
   Boundary("detrital_2")
   {
    z=24;
   };
   Boundary("detrital_1")
   {
    z=14;
   };
   Date("bh04",N(calBP(-51),5.3))
   {
    z=9.3;
   };
   Date("top",U(calBP(-72),calBP(-60)))
   {
    z=0;
   };
   Boundary();
  };
 };
```

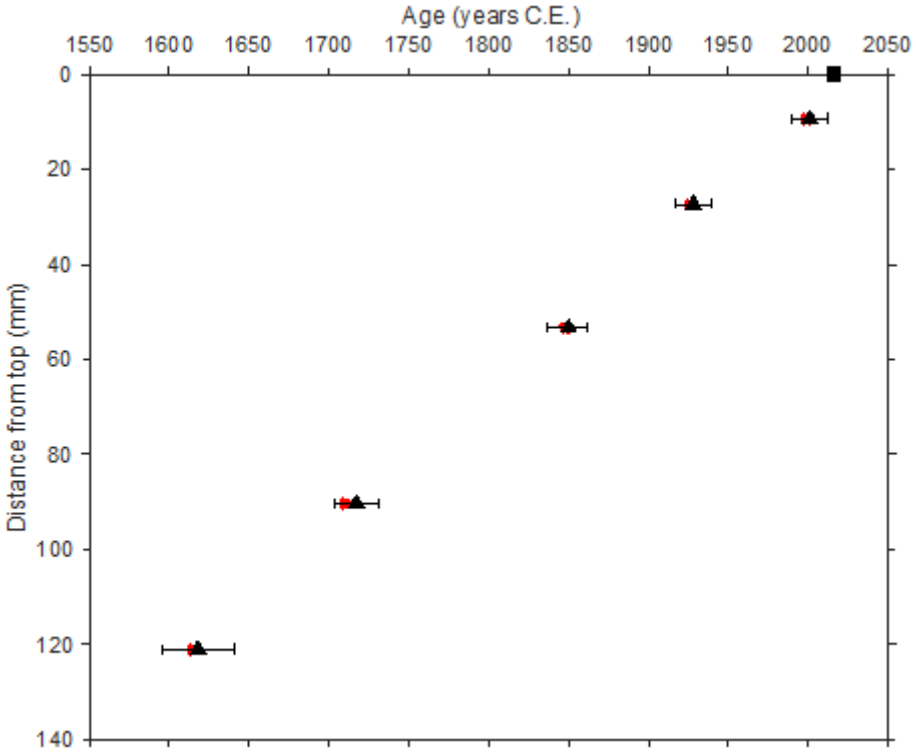

Figure S2. Age-depth plot of stalagmite MAYA-22-7. Black triangles show the mean corrected U-Th age and error bars indicate the 95% confidence interval. Red x's mark the uncorrected U-Th ages. A black rectangle is placed between 2010-2022 C.E., marking the estimated top age of the stalagmite, collected in August 2022.

Table S1: U-Th isotope activity ratios, calculated age (years C.E.), and Monte Carlo derived 95% confidence interval on the age for the five stalagmite MAYA-22-7 U-Th samples. An initial $^{230}Th/^{232}Th$ activity ratio range of 0.1-2 (uniform distribution) was used to correct the ages for initial detrital Th contamination. The ^{234}U and ^{230}Th half-lives used to calculate age are provided in Cheng et al. (2013).

Sample ID	Distance from top (mm)	^{238}U (ppb)	^{232}Th (ppb)	($^{230}Th/^{232}Th$) measured	($^{234}U/^{238}U$) measured	($^{234}U/^{238}U$) 1s	($^{230}Th/^{238}U$) measured	($^{230}Th/^{238}U$) 1s	($^{232}Th/^{238}U$) measured	($^{232}Th/^{238}U$) 1s
bh04	9.3	1097	0.04	17	1.0236	0.0004	0.00022	0.00005	1.254E-05	3E-08
bh02	27.3	1322	0.09	43	1.0369	0.0006	0.00092	0.00005	2.134E-05	3E-08
bh05	53.3	1202	0.07	92	1.0435	0.0005	0.00167	0.00006	1.805E-05	4E-08
bh01	90.3	1181	0.22	50	1.0338	0.0005	0.00296	0.00006	5.905E-05	5E-08
bh03	121.0	1133	0.11	119	1.0330	0.0005	0.00386	0.00011	3.237E-05	7E-08

Sample ID	Year measured (years CE)	Initial ($^{230}Th/^{232}Th$)	Age uncorrected (years CE)	95% CI lower	95% CI upper	Age corrected (years CE)	95% CI lower	95% CI upper
bh04	2022.83	0.1-2	1999	1989	2010	2001	1990	2011
bh02	2022.83	0.1-2	1926	1915	1936	1928	1918	1939
bh05	2022.83	0.1-2	1848	1836	1861	1850	1838	1863
bh01	2022.83	0.1-2	1710	1698	1722	1717	1703	1731
bh03	2022.83	0.1-2	1615	1592	1637	1618	1595	1641

Table S2: OxCal modelled ages of the 10 biomarker samples.

Sample #	Position	Distance from top (mm)	OxCal modelled mean age (years CE)	Error 2σ (years)
4	pit top	0.5	2015	6
4	pit bottom	4.1	2009	8
3	pit top	4.6	2009	8
3	pit bottom	9.1	2001	10
5	pit top	9.6	2000	11
5	pit bottom	13.0	1994	19
2	pit top	15.0	1986	21
6	pit top	15.0	1986	21
6	pit bottom	19.1	1965	19
2	pit bottom	19.1	1965	19
8	pit top	23.2	1944	17
8	pit bottom	23.2	1944	17
9	pit top	25.1	1936	15
9	pit bottom	30.8	1918	11
1	pit top	35.6	1903	11
1	pit bottom	39.1	1892	11
10	pit top	44.8	1874	11
10	pit bottom	50.8	1855	11
11	pit top	70.3	1788	12
11	pit bottom	78.7	1759	12

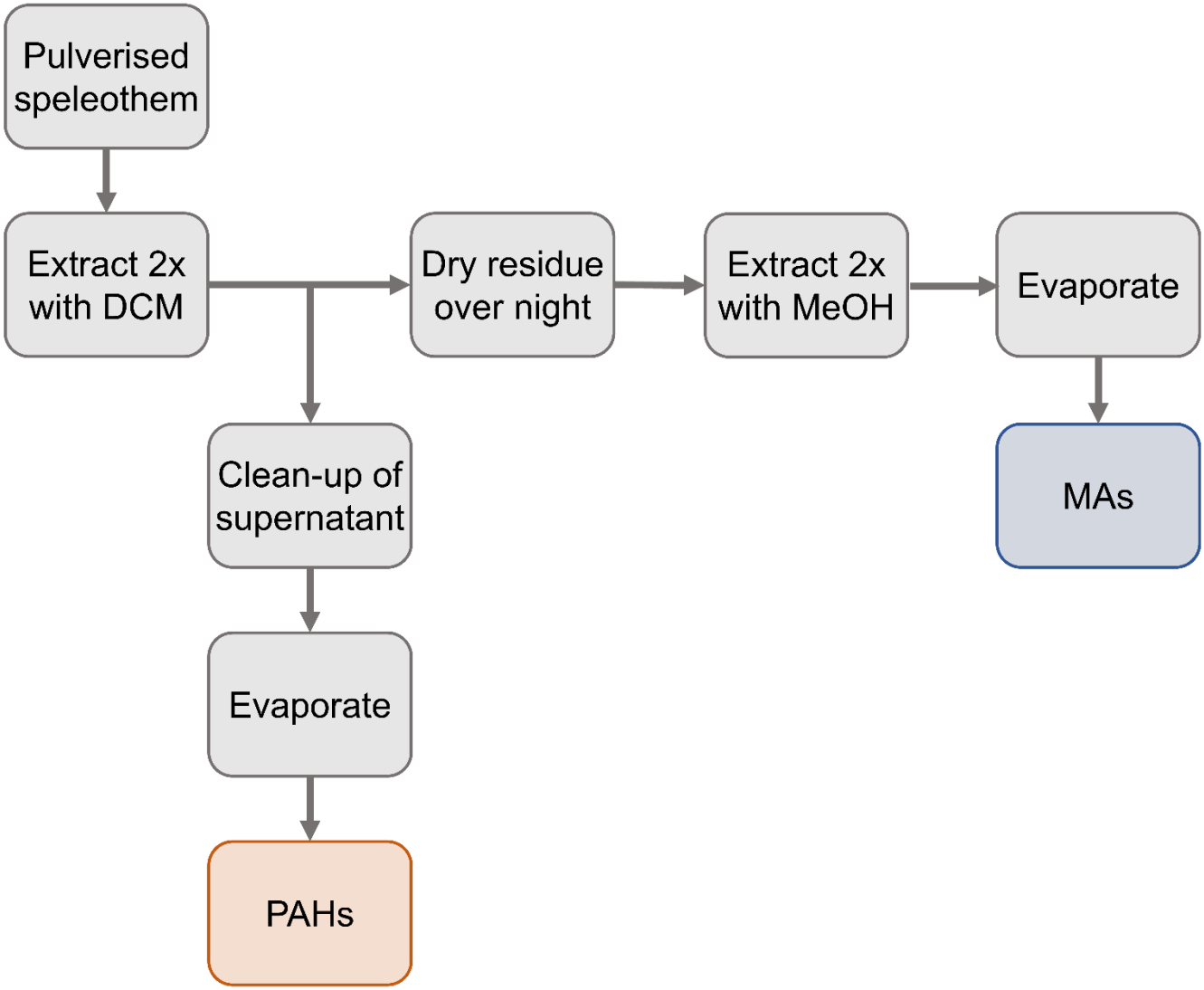

Figure S3: Flow chart of the sample preparation method.

Table S3: Determined d-PAH and ^{13}C-levoglucosan recoveries (%) of the 10 samples from stalagmite MAYA-22-7 from Cenote Ch'en Mul, Mayapan.

Age (Year CE)*	**2010-2015**	**2000-2010**	**1995-2000**	**1945-1985**	**1945-1965**	**1920-1935**	**1890-1905**	**1855-1875**	**1760-1790**	**1640-1650**
Sample #	**4**	**3**	**5**	**2**	**6**	**8**	**9**	**1**	**10**	**11**
d-NAP	48.1 ±9.8	57.6 ±4.2	101.7 ±36.4	48.9 ±3.5	67.4 ±19.7	41.6 ±8.2	82.8 ±26.8	66.6 ±5.0	97.2 ±27.0	60.8 ±16.5
d-ACE	51.6 ±10.5	47.7 ±3.5	120.7 ±43.1	40.7 ±2.9	77.3 ±22.6	45.5 ±9.0	93.8 ±30.3	56.7 ±4.3	101.1 ±28.0	57.4 ±15.5
d-PHE	66.9 ±13.6	76.8 ±5.6	127.2 ±45.5	66.6 ±4.8	89.6 ±26.2	46.4 ±9.1	100.3 ±32.4	88.7 ±6.7	110.0 ±30.5	69.7 ±18.9
13C-LEV	70.7 ±7.6	66.8 ±6.9	79.2 ±1.8	66.1 ±4.5	74.2 ±6.5	61.8 ±4.7	82.9 ±10.2	80.7 ±2.2	71.4 ±17.2	78.1 ±5.2

*: Start and end dates have errors of ± 6-20 years (95 % confidence interval)

Table S4: Determined PAH and MA concentrations (ng g^{-1}) of the 10 samples from stalagmite MAYA-22-7 from Cenote Ch'en Mul, Mayapan.

Age (Year CE)*	**2010-2015**	**2000-2010**	**1995-2000**	**1945-1985**	**1945-1965**	**1920-1935**	**1890-1905**	**1855-1875**	**1760-1790**	**1640-1650**
Sample #	**4**	**3**	**5**	**2**	**6**	**8**	**9**	**1**	**10**	**11**
NAP	1.4 ±0.3	< LOD	3.2 ±1.1	2.8 ±0.2	7.1 ±2.1	1.4 ±0.3	5.2 ±1.7	1.2 ±0.1	4.0 ±1.1	2.2 ±0.6
ACY	0.1 ±0.02	0.3 ±0.02	0.1 ±0.04	0.5 ±0.04	0.3 ±0.1	< LOD	0.3 ±0.1	0.1 ±0.01	0.2 ±0.1	< LOD
ACE	0.2 ±0.05	0.2 ±0.01	0.5 ±0.2	0.3 ±0.02	0.7 ±0.2	0.2 ±0.05	0.5 ±0.2	0.2 ±0.02	0.4 ±0.1	0.3 ±0.1
FLN	0.4 ±0.1	0.4 ±0.03	0.6 ±0.2	0.8 ±0.1	0.7 ±0.2	0.2 ±0.05	0.6 ±0.2	0.4 ±0.03	0.5 ±0.1	0.4 ±0.1
PHE	3.8 ±0.8	3.8 ±0.3	3.9 ±1.4	7.20 ±0.5	5.7 ±1.7	1.8 ±0.4	4.0 ±1.3	3.3 ±0.3	3.9 ±1.1	2.2 ±0.6
ANT	0.1 ±0.01	1.0 ±0.1	0.1 ±0.03	2.1 ±0.2	< LOD	< LOD	< LOD	0.7 ±0.1	< LOD	< LOD
FLT	< LOD	< LOD	0.7 ±0.3	< LOD	< LOD	< LOD	0.7 ±0.2	< LOD	0.7 ±0.2	< LOD
PYR	0.4 ±0.1	0.5 ±0.004	0.6 ±0.2	0.9 ±0.1	0.9 ±0.3	< LOD	0.5 ±0.2	0.7 ±0.05	0.5 ±0.1	0.3 ±0.1
RET	< LOD	< LOD	0.8 ±0.3	< LOD	< LOD	< LOD	0.4 ±0.1	< LOD	< LOD	< LOD
BAA	< LOD	< LOD	< LOD	< LOD	< LOD	< LOD	< LOD	< LOD	< LOD	< LOD
CHR	< LOD	< LOD	< LOD	< LOD	< LOD	< LOD	< LOD	< LOD	< LOD	< LOD
BBF	< LOD	< LOD	< LOD	< LOD	< LOD	< LOD	< LOD	< LOD	< LOD	< LOD
BAP	< LOD	< LOD	< LOD	< LOD	< LOD	< LOD	< LOD	< LOD	< LOD	< LOD
INP	< LOD	< LOD	< LOD	< LOD	< LOD	< LOD	< LOD	< LOD	< LOD	< LOD
DBA	0.1 ±0.02	0.0 ±0.001	0.2 ±0.1	0.1 ±0.004	< LOD	0.02 ±0.004	0.1 ±0.03	0.1 ±0.004	0.04 ±0.01	< LOD
DPE	< LOD	< LOD	< LOD	< LOD	< LOD	< LOD	< LOD	< LOD	< LOD	< LOD
MAN	0.3 ±0.03	0.1 ±0.02	0.3 ±0.02	0.4 ±0.08	0.3 ±0.06	0.3 ±0.01	< LOD	0.1 ±0.02	0.2 ±0.01	0.3 ±0.0003
GAL	0.3 ±0.1	0.1 ±0.02	0.2 ±0.003	0.4 ±0.07	0.7 ±0-01	0.3 ±0.01	0.1 ±0.02	0.1 ±0.01	0.2 ±0.03	0.3 ±0.01

LEV	1.8 ±0.20	0.6 ±0.09	2.3 ±0.001	3.4 ±0.05	5.7 ±0.67	1.9 ±0.02	1.9 ±0.14	0.8 ±0.02	2.0 ±0.42	2.0 ±0.07

*: Start and end dates have errors of ± 6-20 years (95 % confidence interval)

Table S5: Calculated sums and diagnostic ratios of the 10 samples from stalagmite MAYA-22-7 from Cenote Ch'en Mul, Mayapan.

Age (Year CE)*	**2010-2015**	**2000-2010**	**1995-2000**	**1945-1985**	**1945-1965**	**1920-1935**	**1890-1905**	**1855-1875**	**1760-1790**	**1640-1650**
Sample #	**4**	**3**	**5**	**2**	**6**	**8**	**9**	**1**	**10**	**11**
Σ15†	6.4 ±1.3	6.2 ±0.5	9.9 ±3.5	14.7 ±1.1	15.4 ±4.5	3.8 ±0.7	11.9 ±3.8	6.7 ±0.5	10.3 ±2.8	5.4 ±1.5
LMW‡	6.0 ±1.2	5.6 ±0.4	9.0 ±3.2	13.8 ±1.0	14.5 ±4.2	3.7 ±0.7	11.3 ±3.7	6.0 ±0.5	9.7 ±1.4	5.0 ±1.4
HMW◊	0.4 ±0.1	0.5 ±0.04	0.9 ±0.3	0.9 ±0.1	0.9 ±0.3	0.02 ±0.004	0.6 ±0.2	0.7 ±0.1	0.5 ±0.1	0.3 ±0.1
LMW/HMW	13.6 ±5.5	10.4 ±1.5	10.3 ±7.3	14.9 ±2.1	15.8 ±9.2	175.5 ±69.1	19.3 ±12.5	8.5 ±1.3	18.9 ±10.5	14.7 ±8.0
PHE/ANT	74.7 ±30.3	4.0 ±0.6	43.0 ±30.7	3.4 ±0.5	NA	NA	NA	4.8 ±0.7	NA	NA
ANT/(ANT+PHE)	0.01 ±0.01	0.2 ±0.03	0.02 ±0.02	0.2 ±0.03	NA	NA	NA	0.2 ±0.03	NA	NA
RET/(RET+PHE+ANT)	NA	NA	0.16 ±0.18	NA	NA	NA	0.10 ±0.06	NA	NA	NA
LEV/(LEV+Σ15)	0.5 ±0.1	0.2 ±0.04	0.4 ±0.1	0.4 ±0.04	0.5 ±0.2	0.6 ±0.1	0.3 ±0.1	0.3 ±0.03	0.4 ±0.2	0.5 ±0.2
LEV/MAN	5.9 ±1.2	9.7 ±3.8	8.0 ±0.6	9.5 ±2.3	18.8 ±5.7	7.4 ±0.5	NA 18.6	9.1 ±2.1	8.8 ±2.5	6.0 ±0.2
LEV/(MAN+GAL)	3.3 ±0.8	4.7 ±3.0	4.6 ±0.4	4.8 ±2.1	5.9 ±1.8	3.7 ±0.4	±4.96	5.4 ±2.0	4.7 ±2.1	3.1 ±02.

*: Start and end dates have errors of ± 6-20 years (95 % confidence interval) †: Sum of non-alkylated PAHs; ‡: Sum of two and three-ring PAHs; ◊: Sum of four and five-ring PAHs

References

Brown, C. T.: Water Sources at Mayapan, Yucatan, Mexico, in: Precolumbian Water Management: Ideology, Ritual, and Power, edited by: Lucero, L. J., University of Arizona Press, Washington, D. C., 171–186, https://doi.org/10.2307/j.ctv2vt02c0.14, 2006.

Weeks, J. M. and Masson, M.: The Carnegie Maya: II: Carnegie Institution of Washington current reports, 1952-1957, University Press of Colorado, Boulder, Colo, 625 pp., 2009.